

Original Article

# Optimized Convolutional Neural Networks for Detecting Covid-19 from Chest X-Ray

S. Deepa<sup>1</sup>, S. Shakila<sup>2</sup>

<sup>1,2</sup>Department of Computer Science, Government Arts College – Bharathidasan University, Tiruchirappalli, Tamil Nadu, India.

<sup>1</sup>Corresponding Author : [profsdeepa2020@gmail.com](mailto:profsdeepa2020@gmail.com)

Received: 27 July 2022

Revised: 14 October 2022

Accepted: 03 December 2022

Published: 24 December 2022

**Abstract** - COVID-19 is a respiratory syndrome caused by the Severe Acute Respiratory Syndrome Coronavirus-2 (SARS-CoV-2) infection. Typically, COVID-19 is an acute resolved disease with symptoms at onset, such as dry cough, fatigue, fever, or other gastrointestinal symptoms. While COVID-19 has milder clinical symptoms and a lower fatality rate than SARS and MERS, it can also be deadly as patients may develop a diffuse alveolar injury, progressive respiratory failure, etc. Currently, there is the existing infrastructure's (for example, limited image data sources having expert-labelled datasets) inadequacy for identifying COVID-19-positive patients. Also, a lot of time is consumed due to manual detection. With the increase in global incidences, there is an expectation that a deep learning-based solution will soon be developed and incorporated with clinical practices to offer an easy, accurate, and cost-effective process for the automated recognition of COVID-19 assistance of the screening procedure. Convolutional Neural Networks (CNN) are effective in identifying COVID-19. The deep learning models require to have proper hyperparameters to perform efficiently. In this work, the hyperparameters of CNN are optimized with methods of hybrid optimization based on the Firefly Algorithm (FA) and the Particle Swarm Optimization (PSO) algorithms to boost the diagnostic performance.

**Keywords** - Covid-19, Convolutional Neural Networks, Firefly Algorithm, Particle Swarm Optimization (PSO), Sars-cov-2.

## 1. Introduction

The coronavirus (2019-nCoV) infection emerged in Wuhan, China, in December 2019. Later, it rapidly spread across China and various countries and became a global health concern affecting millions worldwide. The World Health Organization (WHO) announced that the epidemic disease caused by the 2019-nCoV would be hereafter referred to as the coronavirus disease (COVID-19). Studies have progressively demonstrated human-to-human transmission of COVID-19 via direct contact or droplets. Furthermore, yet another study had presumed their suspicions that 41% of the patients were suffering from the hospital-related transmission of COVID-19. In addition, evidence of a rapid increase in the incidence of infections and the possibility of transmission by asymptomatic carriers strongly suggested that the SARS-CoV-2 had effective transmission amongst humans and exhibited high potential for turning into a pandemic [1].

COVID-19's clinical course can range from asymptomatic infection or mild respiratory symptoms to severe or life-threatening pneumonia and even death. Since there is no insight into a definitive curative treatment, and the vulnerable population is prone to a high rate of mortality,

the health authorities have tried to reduce risks and also to focus on available drugs for the development, timely as well as cost-effective strategies of medical therapy for the patients who were hospitalized as well as critically ill. Numerous antiviral/antimalarial agents like remdesivir, hydroxychloroquine, chloroquine, and immuno-modulating therapies were evaluated in various countries to gauge their safety and safety efficacy in treating COVID-19 [18]. Remdesivir started to laude as a possible candidate drug for the COVID-19 treatment as certain studies had shown promising results. The Rapid Diagnostic Test (RDT) is a fast detection test based on antibody type of testing, and also can yield results within a time period of 30 minutes. Even so, the RDT test kits have limited availability, and their success depends on the sample quality and the illness' onset time. In addition, the test is not recommended for COVID-19 diagnosis as it does offer false positive results due to its inability to discriminate COVID-19 from other viral infections. Reverse Transcription Polymerase Chain Reaction (RT-PCR) is another popularly used viral test.

As the first-line option for screening, the RT-PCR [3] is employed as the gold-standard tool. Nonetheless, its sensitivity is only between the 50-62% range, as demonstrated through various studies. It will imply that there



is a possibility of getting an initial negative RT-PCR result. Multiple RT-PCR tests are required to ensure the test result's correctness over an observational period of 14- days. Unfortunately, this is quite trying for the patient and also expensive.

Since the respiratory system is the prime target of COVID-19, a vital tool for diagnosis as well as early disease management has been chest radiology scans. Chest X-rays are employed as a first-line diagnostic tool in Italy and multiple countries. It is possible to effectively ascertain details related to the lung condition as well as the different phases of either illness or recovery with the use of radiology scans. Chest X-ray is an extensively available tool in most clinical settings; it is less time-consuming regarding patient preparation and diagnosis. As a result, it is possible to employ CXR for patient triage, determining patient treatment priority, and medical resource utilization.

With the use of deep learning techniques in the medical imaging domain, significant improvements have been accomplished in the performance of image analysis. Deep learning is now increasingly used to assist radiologists in diagnosing various medical conditions using images like x-ray, CT, MRI, etc. Many studies have demonstrated the effectiveness of Deep learning in the medical domain. The architecture of deep learning algorithms is more complex than machine learning algorithms. The deep learning architecture extracts the features from the input image and processes them to classify them into various classes as trained. Convolutional Neural Networks (CNNs) are often employed in diagnosing a medical condition using medical images. CNN has diverse architectures as well as applications in various fields. Thus, right from the pandemic's first few months, there has been a comprehensive investigation into the application of deep learning methods for detecting COVID-19 from X-rays.

This work aims to use deep learning for COVID-19 diagnosis using x-ray images. The contributions of this work are three-fold,

- Evaluate Deep learning methods for COVID-19 diagnosis.
- To optimize the hyperparameters of CNN.
- Enhance the deep learning techniques using the PSO-CNN, the FA-CNN, and the hybrid FA-PSO CNN algorithm.

Most of the work on COVID-19 deals with the treatment, Li et al. [4] investigated the effects of remdesivir for treating COVID-19. Laboratory experiments and reports from compassionate use are presented. The safety and effect of remdesivir in humans were studied. It was concluded that clinical trials for further clarification are required. Cao et al. [5] analyzed the pharmacological actions and previous

attempts of remdesivir for treating COVID-19. The authors presented the structure, immunogenicity, and pathogenesis of coronavirus infections of the novel coronavirus.

Chiotos et al. [6] studied the effects of COVID in paediatrics. Physicians from 20 different geographical places convened to investigate pediatric infectious diseases. A web-based survey was conducted to collect the relevant information, and a set of guidance statements was developed. Gordon et al. [7] expressed and purified active SARS-CoV-2 RNA-dependent RNA polymerase (RdRp) composed of the nonstructural proteins nsp8 and nsp12. Ardabili et al. [19] presented a comparative analysis of machine learning and soft computing methods for predicting the COVID-19 outbreak as an alternative to Susceptible-Infected-Recovered (SIR) and Susceptible-Exposed-Infectious-Removed (SEIR) models. The investigation concluded that the Multi-Layered Perceptron (MLP); and Adaptive Network-Based Fuzzy Inference System (ANFIS) had shown better efficiency in classifying COVID-19 from the medical images.

This work has proposed the optimized CNN (the PSO-CNN, the FA-CNN, and the hybrid FA-PSO CNN) algorithm for detecting COVID-19. The subsequent sections will organize the remaining investigation portion as follows: Section two will elaborate on this work's numerous utilized methods. While Section three will describe the experimental results, Section four will conclude the work.

## 2. Methodology

### 2.1. Convolutional Neural Networks (CNN)

CNN is a powerful tool for image classification. Dilbag Sing et al. described the structure and useful feature extraction characteristics involved in turning an image transform into the CNN as a dynamic model for image classification purposes. The authors observed that the CNN layers were organized into three distinct dimensions: width, height, and depth. Only a limited number of neurons would get attached by the given layer's neurons. For the CNN's output, there is a need to mitigate the probability score vector as well as the depth dimension coordination [9, 10].

Features extracted from chest images can be employed to accurately classify whether or not the patients are Covid-19 infected or not. Disease detection with the CNN model's utilization is effective. The following points will explain the CNN layers in detail:

- Convolutional Layer: Being the fundamental building block of the Convolutional Neural Network, this layer will carry out all the computational works. Three distinct parameters will determine the depth, stride, and padding. Equation 1 will express the convolutional layer's output size as follows:

$$o = \left(\frac{n+2p-f}{s} + 1\right) x \left(\frac{n+2p-f}{s}\right) \quad (1)$$

In which o = output size (width\*height), n = image width = image height, s = stride, p = padding, and f = number of filters.

- Max Pooling Layer: The input features' non-overlapping sub-regions will employ a max filter for the Max-pooling development. With Max-pooling, it may be possible to minimize the features' dimensionality. A Max-Pooling layer's output size is computed as per Equation 2:

$$o = \left(\frac{nw-f}{s} + 1\right) x \left(\frac{nh-f}{s}\right) \quad (2)$$

Here, nh = input height, nw = image width.

- Dropout Layer: A dropout layer will offer a random probability with zero input elements. Upon utilization of the dropout method, there may be an increase in the over-fit on the neural networks algorithm.

- Fully Connected Layer: This layer will denote a feature vector for the input. In turn, the feature vector will save the significance of information for the input.

- Softmax Layer: This layer will display the decimal probabilities in multi-class classifications. The sum of this layer's probability will always have 1.0 as its end result.

The performance of the CNN depends on parameters like batch size, learning rate, activation, and the number of epochs. This work optimises these hyperparameters using metaheuristics like PSO and FF algorithms.

## 2.2. Particle Swarm Optimization (PSO)-CNN

PSO accomplishes the optimal solution by replicating the social behaviours of schools of fish as well as bird flocks. This algorithm has had successful application in diverse real-world applications due to its computational efficiency in resolving problems of complex optimization problems as well as the quick convergence towards an acceptably good solution [11].

The PSO algorithm will commence with a set of randomly generated solutions of m particles within the D-dimension solution space.

$X_i(x_i^1, x_i^2, \dots, x_i^D)$  indicate the particles' position (direction) and  $V_i = (v_i^1, v_i^2, \dots, v_i^D)$  the velocity. Every X position in the flock is evaluated based on the objective function. While personal best (pbest) will indicate, the current generation's local best for every particle, the global best (gbest) will indicate the global best amongst the current generation's local best examples. Every particle will shift

towards the direction of its previous best ( $p_{id}$ ) and the global best (pgd) position in the swarm with a specific velocity to detect the gbest position. The below Equations 3 and 4 will express the updating of the particle's velocity as well as position [20]:

$$v_{id}^{k+1} = wv_{id}^k + c_1r_1(p_{id}^k - x_{id}^k) + c_2r_2(p_{gd}^k - x_{id}^k) \quad (3)$$

$$x_{id}^{k+1} = x_{id}^k + v_{id}^{k+1}; \quad i = 1,2,3,\dots,m; \quad d = 1,2,3,\dots,D \quad (4)$$

In the aforementioned equation, w will indicate the inertia weight employed to balance the algorithm's local and global search abilities, and  $c_1$  and  $c_2$  will be the acceleration coefficients showing the learning behaviour.  $r_1$  and  $r_2$  will indicate uniform random numbers which range from 0 to 1,  $p_{id}^k$  will indicate the personal best position of particle i in the d<sup>th</sup> dimension, k will indicate the number of iterations,  $x_{id}^k$  will indicate the position, and  $p_{gd}^k$  will indicate the gbest position accomplished so far in the flock.

The work has implemented the PSO algorithm onto the CNN architecture to design a CNN architecture with an optimized hyperparameter for classifying chest x-rays as COVID-19 or Normal. Hence, it will have to resolve a problem with a number of factors which will express the CNN's hyper-parameters whilst also ensuring a high classification accuracy. There are numerous hyper-parameters involved in defining a CNN architecture. This work will focus on optimising the batch size, learning rate, activation, and the number of the epoch that forms the CNN structure. The fitness function is based on classification accuracy such that its goal is to identify the ideal hyper-parameter values with less error as well as higher accuracy [13].

After the random generation of the initial population, the fitness function will be set as the CNN's classification accuracy. If there has not been any occurrence of a change in the individual hyper-parameters, there will be no need for the CNN to be re-trained. There is a repetition of this procedure till the iteration numbers have ended. Below are the steps of the proposed method:

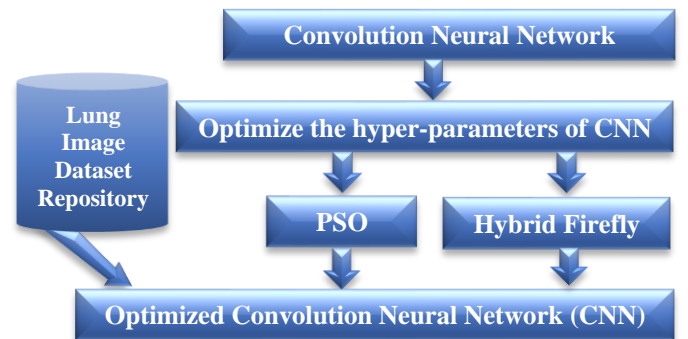


Fig. 1 Flow of Investigation

Initialize the PSO's parameters (i.e., size of the population, number of iterations, c1 and c2).

- Step 1: Set the particles' position as well as velocity to correspond with the random CNN hyper-parameters (batch size, learning rate, activation, number of epochs)
- Step 2: Train the CNN with the parameter values for all the particles.
- Step 3: Evaluate the fitness value (i.e., classification accuracy) for all the particles. Later, pick the pbest as well as the swarm's best particle position.
- Step 4: Update each particle's position, X, and velocity, V.
- Step 5: End this procedure and CNN's model with the optimized parameters if the iteration numbers have been completed. Otherwise, go back to Step 3 to repeat the process.

### 2.3. Firefly CNN

In 2008, Yang introduced the Firefly Algorithm (FA) as a swarm intelligence metaheuristic. In recent times, it has been a very popular metaheuristic and also has undergone specific new improvements. The FA metaheuristic has been successfully applied in diverse tasks [21]. The FA metaheuristic will model the group behaviour of fireflies. This approach's basic assumption is that every firefly (solution) will shift towards the direction of a brighter (i.e., more attractive) firefly. The below-mentioned idealized rules so as to model the firefly group's behavior and also incorporate it into an optimization algorithm: a) The population's fireflies are all unisex; b) there is a directly proportional relationship between the attractiveness as well as the brightness; c) the objective function's value decides the brightness. For maximization, the definition of a solution's brightness at a specified location x can be given as  $I(x) \sim f(x)$ , in which  $I(x)$  will indicate the attractiveness, and  $f(x)$  will indicate the objective function's value at this particular location. For the case of problems of minimization, there is the usage of the below Equation 5:

$$I(x) = \begin{cases} \frac{1}{f(x)}, & \text{if } f(x) > 0 \\ 1 + |f(x)|, & \text{otherwise} \end{cases} \quad (5)$$

An increase in the light intensity, as well as attractiveness, will result in a decrease in the distance from the source and vice-versa. Equation 6 will express this observation as below:

$$I(r) = \frac{I_0}{1+\gamma r^2} \quad (6)$$

In the above equation,  $I(r)$  will indicate the light intensity,  $r$  will indicate the distance, and  $I_0$  will indicate the light intensity at the source. Additionally, the parameter  $\gamma$  will model the air absorption. For the majority of FA implementations in the published literature, the below

Gaussian form, Equation 7, can be used for approximation of the combined effect of the inverse square law as well as the absorption:

$$I(r) = I_0 e^{-\gamma r^2} \quad (7)$$

The attractiveness,  $\beta$ , will vary with the distance  $r_{i,j}$  which is between solutions  $i$  and  $j$ . Also, as per below Equation 8, it is in direct proportion to the solutions' light intensity:

$$\beta(r) = \beta_0 e^{-\gamma r^2} \quad (8)$$

Wherein,  $\beta_0$  will indicate the attractiveness at  $r = 0$ . Equation 4 will determine a characteristic distance,  $\Gamma = 1/\sqrt{\gamma}$ , over which the attractiveness will experience a significant change from  $\beta_0$  to  $\beta_0 e^{-1}$ .

The majority of the practical implementations will replace the aforementioned expression with Equation 9 so as to mitigate the usage of computational resources - a very critical point for the hyper-parameter optimization of CNNs:

$$\beta(r) = \frac{\beta_0}{1+\gamma r^2} \quad (9)$$

The below Equation 10 is used by every solution in the population  $i$  in each iteration of the algorithm's execution to shift towards a better solution  $j$ :

$$x_i(t+1) = x_i(t) + \beta_0 r^{-\gamma r_{i,j}^2} (x_j - x_i) + \alpha(\kappa - 0.5) \quad (10)$$

Here,  $\beta_0$  will indicate the attractiveness at  $r = 0$ ,  $\alpha$  will indicate the randomization parameter,  $\kappa$  will indicate a pseudo-random number within the  $[0; 1]$  range, and  $r_{i,j}$  will indicate the distance between solutions  $i$  as well as  $j$ . The Cartesian distance concept is employed in following Equation 11 to measure the distance between solutions  $i$  and  $j$ :

$$r_{i,j} = ||x_i - x_j|| = \sqrt{\sum_{k=1}^D (x_{i,k} - x_{j,k})^2} \quad (11)$$

In the above equation,  $D$  will indicate the number of problem parameters.

### 2.4. Proposed Hybrid Firefly CNN

As the FA has no capability for memory, an attempt has been made to hybridize the FA as well as the PSO. It is evident from earlier works that the PSO is one of the most well-known global search methods. Thus, combining the FA and the PSO will identify a better solution for the search space's exploration by applying the PSO's ability to memorize its previous best to determine the subsequent probable solutions [15]. The proposed Hybrid Firefly CNN will commence with the execution of the FA. All the fireflies

will start to shift towards other brighter fireflies. Upon its completion, each firefly's fitness will be compared with its preceding firefly to acquire the *pbest*. Afterwards, the FA procedure will continue until the termination criteria are fulfilled. At this point, there is the acquisition of an optimal solution, and the procedure will be brought to a halt. Otherwise, the FA procedure will be re-iterated until the termination criteria are fulfilled.

With the hybridization of FA and PSO, it is possible to overcome the FA's memorizing capability compared to the PSO. This work has used the PSO's ability to memorize the solutions' previous best location to update the next value within the search space. Better solutions are obtained by utilising the previous best place (*pBest*) in the previous iteration to update the next value [16]. The firefly's current position, *xi*, is a coordinate set which will denote a point within the search space. A firefly will indicate the problem's solution set. The algorithm will compare the firefly's attractiveness when it tries to shift towards the new position, and the value will get stored in *pBest*; otherwise, the firefly will continue to stay in its current position. The *pBest* value will get compared at a later iteration for the determination of optimal solutions.

The algorithm will update the light intensity (*I*) based on the *pBest* to continue finding the fireflies' better positions. Selection of new points will be made via adjustment of the randomization factor as a step size. It is possible to terminate the FA procedure in the following two distinct ways: while the one way is to terminate based on an arbitrary predefined number of iterations, the second way is done on the basis of a predefined value of fitness. This research will employ a predefined number of iterations as the proposed algorithm's termination criteria. The algorithm will come to a halt upon the fulfilment of a maximum number of iterations. Evaluation of the fitness values will be done on the basis of the optimal solution, which is represented by the fireflies.

The proposed Hybrid Firefly CNN algorithm can be detailed as follows: Initially, the input parameters will be inserted, which will be employed by both algorithms. Later, uniform particle vectors will be prepared randomly in the predefined search and velocity ranges. There will be evaluation as well as assignment of the global best (*gbest*) and personal best (*pbest*) particles. The consequent comparison stage will compare if the particle has improved in its fitness value in the previous iteration as per Equation 13. Then, the current position will get saved in a temporary variable (*X<sub>i temp</sub>*). Also, there will be an evaluation of the new position as well as velocity in accordance with Equations 14 and 15:

$$w = w_i - ((w_i - w_f)/iteration_{max}()) \quad (12)$$

$$f(i, t) = \begin{cases} true, & \text{if } fitness(particle_i^t) \leq gbest^{t-1} \\ false, & \text{if } fitness(particle_i^t) > gbest^{t-1} \end{cases} \quad (13)$$

$$X_i(t + 1) = X_i(t) + B_0 e^{-\gamma r_{ij}^2} (X_i(t) - gbest^{t-1}) + a \epsilon_i \quad (14)$$

$$V_i(t + 1) = X_i(t + 1) - X_{i\_temp} \quad (15)$$

Therefore, if a particle has a fitness value that is either better or equivalent to the previous global best, the assumption will be that there is the local search's commencement. An imitative FA will handle the particle. Otherwise, the particle's handling will be done by the PSO, and this PSO will use Equations 3 and 4 to carry on with its standard procedures on the particle. The fitness function evaluations and range limitations will check for all particles and fireflies in the subsequent comparison stage. Upon arriving at the maximum iteration limit, the hybrid algorithm will terminate, and the values of *gbest* and its fitness will be offered as the proposed hybrid algorithm's output.

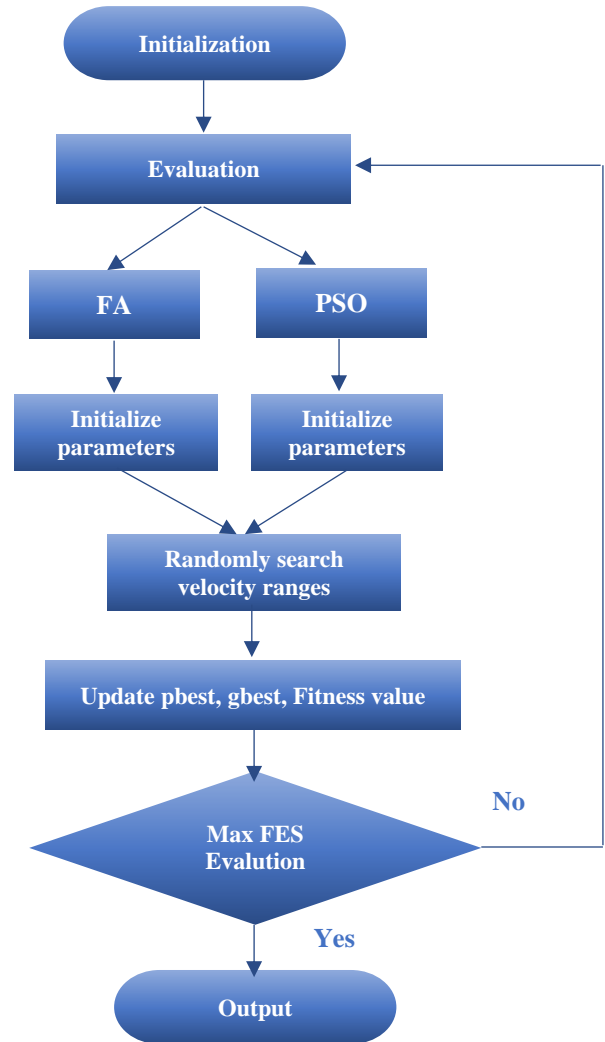


Fig. 2 Flowchart of Proposed Hybrid Firefly

The maximum number of fitness function evaluations (MaxFES) will be utilised. In evolutionary computing, *MaxFES* is a well-known criterion of termination which will allow for the maximum calculation of objective functions. With the parameter of inertia weight ( $w$ ), it is possible to strike a balance in the PSO between the exploration as well as the exploitation. In accordance with Equation 12, there will be utilization as well as assessment of a linear decreasing inertia weight. There will be the employment of a particle's minimum ( $V_{min}$ ) as well as maximum velocities ( $V_{max}$ ) to limit the next distance in a direction. These parameters will get randomly prepared in the velocity range at the proposed algorithm's start.

### 3. Result and Discussion

The proposed methods were evaluated using the chest x-ray. (Figures 3 to 8) shows the sample input image and the visualization of convolutional layer feature maps. Table 1 and (Figures 9 to 11) show the classification accuracy, sensitivity and specificity, respectively.

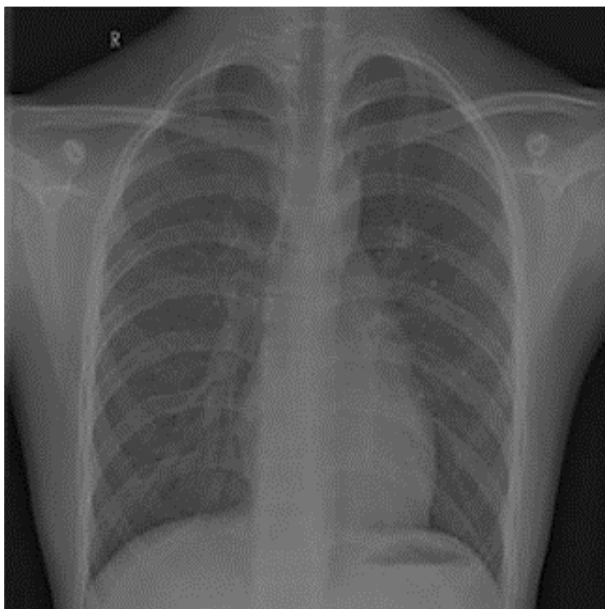


Fig. 3 Sample Image 1

(Figure 3) shows one of the input sample images used in the investigation. (Figures 4 to 8) the feature maps obtained from convolution layers.

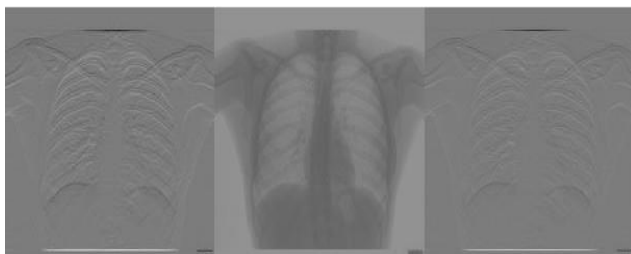


Fig. 4 Output at the first Convolution layer



Fig. 5 Output at the second Convolution layer

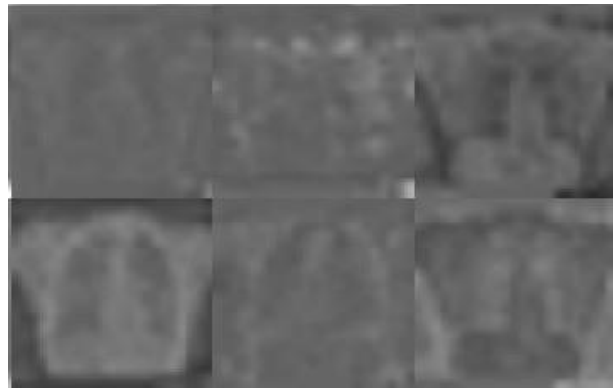


Fig. 6 Output at the third Convolution layer

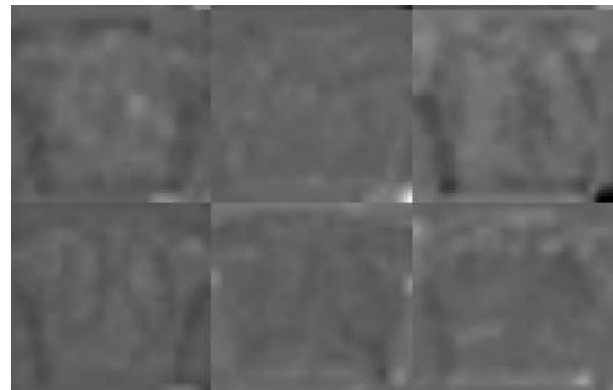


Fig. 7 Output at the fourth Convolution layer

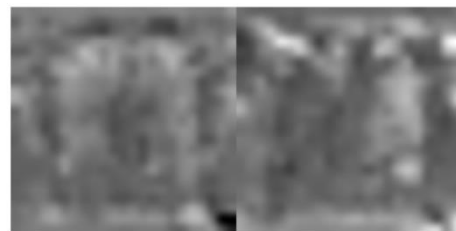


Fig. 8 Output at the fifth Convolution layer

Table 1. Classification Accuracy for Hybrid Firefly CNN

Methods	Classification Accuracy
CNN-3 layer	91.21
CNN-5 Layer	92.1
CNN -7 Layer	95.37
PSO CNN	96.07
Firefly CNN	96.96
Hybrid Firefly CNN	97.34



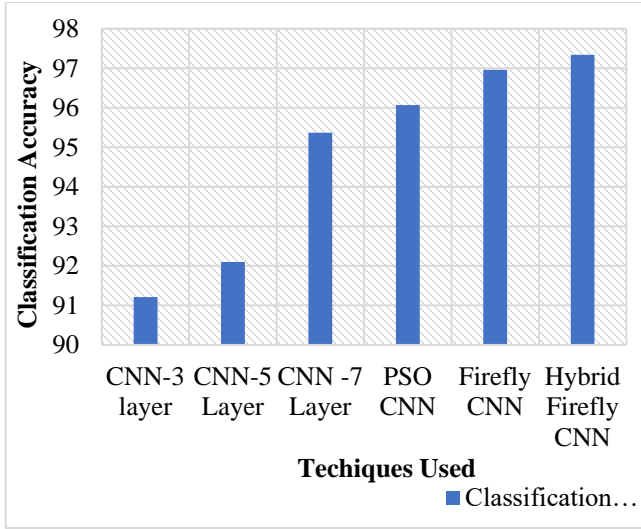


Fig. 9 Classification Accuracy for Hybrid Firefly CNN

Table 2. Sensitivity for Hybrid Firefly CNN

Methods	Sensitivity for Non Covid	Sensitivity for Covid
CNN-3 layer	0.9273	0.8878
CNN-5 Layer	0.9379	0.8939
CNN-7 Layer	0.9879	0.8988
PSO CNN	0.9871	0.9183
Firefly CNN	0.9879	0.9402
Hybrid Firefly CNN	0.9886	0.9488

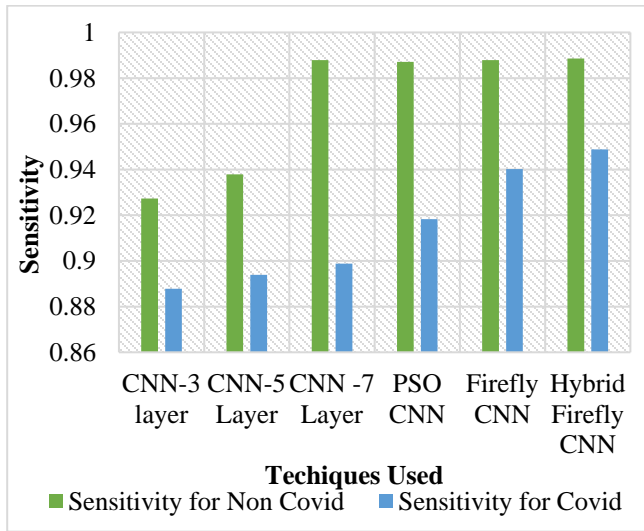


Fig. 10 Sensitivity for Hybrid Firefly CNN

From (Figure 9), it can be observed that the hybrid Firefly CNN has higher classification accuracy by 6.5% for the CNN layer, 5.53% for the CNN-5 layer, 2.04% for the CNN-7 layer, 1.31% for PSO CNN and 0.39% for firefly CNN respectively.

From (Figure 10), it can be observed that the hybrid Firefly CNN has higher sensitivity for non-covid by 6.39%

for the CNN-3 layer, 5.26% for the CNN-5 layer, by 0.07% for the CNN-7 layer, by 0.15% for PSO CNN and by 0.07% for firefly CNN respectively. The hybrid firefly CNN has higher sensitivity for covid by 6.64% for the CNN-3 layer, by 5.95% for the CNN-5 layer, by 5.41% for the CNN-7 layer, by 3.26% for PSO CNN, and by 0.91% for firefly CNN respectively.

From (Figure 11), it can be observed that the hybrid Firefly CNN has a higher specificity for non-covid by 6.64% for the CNN-3 layer, by 5.95% for the CNN-5 layer, by 5.41% for the CNN-7 layer, by 3.26% for PSO CNN and by 0.91% for firefly CNN respectively. The hybrid firefly CNN has a higher specificity for covid by 6.39% for the CNN-3 layer, by 5.26% for the CNN-5 layer, by 0.07% for the CNN-7 layer, by 0.15% for PSO CNN and by 0.07% for the firefly CNN respectively.

It is evident from the experimental results that the proposed hybrid firefly CNN is effective in classifying the x-ray as Covid or Non-Covid compared to other existing CNNs. The combination of the FA and PSO can identify a better solution from the search space's exploration by applying the PSO's ability to memorize its previous best to determine the subsequent probable solutions, thus, achieving the optimal hyperparameters for CNN.

Table 3. Specificity for Hybrid Firefly CNN

Methods	Specificity for Non-Covid	Specificity for Covid
CNN-3 layer	0.8878	0.9273
CNN-5 Layer	0.8939	0.9379
CNN-7 Layer	0.8988	0.9879
PSO CNN	0.9183	0.9871
Firefly CNN	0.9402	0.9879
Hybrid Firefly CNN	0.9488	0.9886

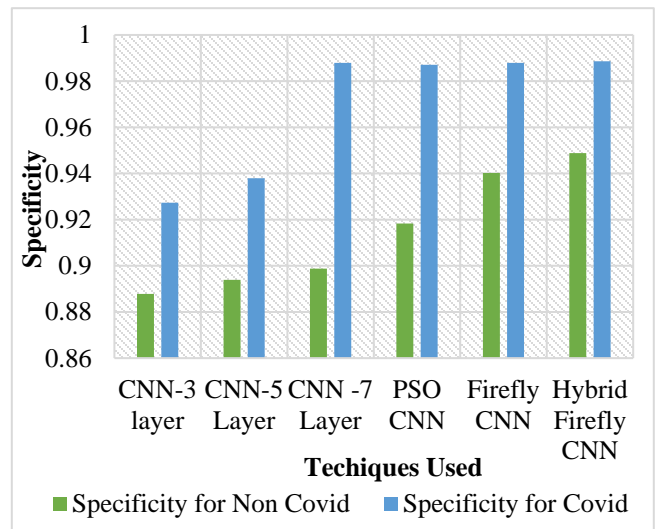


Fig. 11 Specificity for Hybrid Firefly CNN

#### 4. Conclusion

There is an urgent need to develop other patient identification methods due to the limited availability of testing for the presence of the SARS-CoV-2 virus and the concerns about the currently-used methods' accuracy. With earlier studies demonstrating a correlation between specific laboratory tests and diagnosis, it is possible to recommend an alternative approach based on an ensemble of tests. In the field of medical imaging, deep learning has been able to accomplish highly advanced performance. Even so, these disease detection methods solely target boosting the accuracy of either classification or predictions without quantifying a decision's uncertainty. Knowing how much confidence there is in a computer-based medical diagnosis is essential to gain

the clinicians' trust in the technology and enhancing the treatment. Globally, the present key challenge to healthcare is the 2019 Coronavirus (COVID-19) infections. This work has given the proposals for the PSO-CNN, the FA-CNN, and the hybrid FA-CNN methods. The proposed algorithm has the ability to exploit the strong points of the mechanisms of particle swarm as well as FA. Hybrid FA-PSO will check the earlier values of the global best fitness attempt to determine the local search procedure's start properly. Results show that the hybrid Firefly CNN has higher classification accuracy by 6.5% for the CNN-3 layer, 5.53% for the CNN-5 layer, 2.04% for the CNN-7 layer, 1.31% for PSO CNN and by 0.39% for firefly CNN respectively.

#### References

- [1] Chih-Cheng Lai et al., "Severe Acute Respiratory Syndrome Coronavirus 2 (SARS-Cov-2) and Coronavirus Disease-2019 (COVID-19): The Epidemic and the Challenges," *International Journal of Antimicrobial Agents*, vol. 55, no. 3, p. 105924, 2020. *Crossref*, <https://doi.org/10.1016/j.ijantimicag.2020.105924>
- [2] S. Farjana Farvin, and S. Krishna Mohan, "A Comparative Study on Lung Cancer Detection using Deep Learning Algorithms," *SSRG International Journal of Computer Science and Engineering*, vol. 9, no. 5, pp. 1-4, 2022. *Crossref*, <https://doi.org/10.14445/23488387/IJCSE-V9I5P101>
- [3] Hanan S. Alghamdi et al., "Deep Learning Approaches for Detecting COVID-19 from Chest X-Ray Images: A Survey," *IEEE Access*, vol. 9, pp. 20235-20254, 2021. *Crossref*, <https://doi.org/10.1109/ACCESS.2021.3054484>
- [4] Ziyi Li et al., "Rapid Review for the Anti-Coronavirus Effect of Remdesivir," *Drug Discoveries & Therapeutics*, vol. 14, no. 2, pp. 73-76, 2020. *Crossref*, <https://doi.org/10.5582/ddt.2020.01015>
- [5] Yu-Chen Cao, Qi-Xin Deng, and Shi-Xue Dai, "Remdesivir for Severe Acute Respiratory Syndrome Coronavirus 2 Causing COVID-19: An Evaluation of the Evidence," *Travel Medicine and Infectious Disease*, vol. 35, p. 101647, 2020. *Crossref*, <https://doi.org/10.1016/j.tmaid.2020.101647>
- [6] Kathleen Chiotos et al., "Multicenter Initial Guidance on the Use of Antivirals for Children with Coronavirus Disease 2019/Severe Acute Respiratory Syndrome Coronavirus 2," *Journal of the Pediatric Infectious Diseases Society*, vol. 9, no. 6, pp. 701-715, 2020. *Crossref*, <https://doi.org/10.1093/jpids/piaa045>
- [7] Calvin J Gordon et al., "Remdesivir is a Direct-Acting Antiviral that Inhibits RNA-Dependent RNA Polymerase from Severe Acute Respiratory Syndrome Coronavirus 2 with High Potency," *Journal of Biological Chemistry*, vol. 295, no. 20, pp. 6785-6797, 2020. *Crossref*, <https://doi.org/10.1074/jbc.RA120.013679>
- [8] Sagnik M, and Ramaprasad P, "Comparative Study of Convolutional Neural Networks," *SSRG International Journal of Electronics and Communication Engineering*, vol. 6, no. 8, pp. 18-21, 2019. *Crossref*, <https://doi.org/10.14445/23488549/IJECE-V6I8P103>
- [9] Irma Permata Sari et al., "A Basic Concept of Image Classification for Covid-19 Patients Using Chest CT Scan and Convolutional Neural Network," *2020 1st International Conference on Information Technology, Advanced Mechanical and Electrical Engineering (ICITAMEE)*, *IEEE*, pp. 175-178, 2020. *Crossref*, <https://doi.org/10.1109/ICITAMEE50454.2020.9398462>
- [10] Farjana Farvin S, and Krishna Mohan S, "A Comparative Study on Lung Cancer Detection using Deep Learning Algorithms," *SSRG International Journal of Computer Science and Engineering*, vol. 9, no. 5, pp. 1-4, 2022. *Crossref*, <https://doi.org/10.14445/23488387/IJCSE-V9I5P101>
- [11] Neeraj Kumar Jarouliya, and Dr. Nirupama Tiwari, "Utilization of Particle Swarm Optimization (PSO) Use as Clustering Algorithm in MANET," *SSRG International Journal of Computer Science and Engineering*, vol. 6, no. 11, pp. 10-14, 2019. *Crossref*, <https://doi.org/10.14445/23488387/IJCSE-V6I11P103>
- [12] Bindhu J S, and Pramod K V, "A Novel Approach for Satellite Image Classification using Optimized Deep Convolutional Neural Network," *International Journal of Engineering Trends and Technology*, vol. 70, no. 6, pp. 349-365, 2022. *Crossref*, <https://doi.org/10.14445/22315381/IJETT-V70I6P236>
- [13] Zainab Fouad et al., "Hyper-Parameter Optimization of Convolutional Neural Network Based on Particle Swarm Optimization Algorithm," *Bulletin of Electrical Engineering and Informatics*, vol. 10, no. 6, pp. 3377-3384, 2021. *Crossref*, <https://doi.org/10.11591/eei.v10i6.3257>



- [14] Bijaya Kumar Hatuwal, and Himel Chand Thapa, "Lung Cancer Detection Using Convolutional Neural Network on Histopathological Images," *International Journal of Computer Trends and Technology*, vol. 68, no. 10, pp. 21-24, 2020. *Crossref*, <https://doi.org/10.14445/22312803/IJCTT-V68I10P104>
- [15] Nur Farahlina Johari et al., "Machining Parameters Optimization using Hybrid Firefly Algorithm and Particle Swarm Optimization," *Journal of Physics: Conference Series*, IOP Publishing, vol. 892, no. 1, p. 012005, 2017. *Crossref*, <https://doi.org/10.1088/1742-6596/892/1/012005>
- [16] İbrahim Berkan Aydilek, "A Hybrid Firefly and Particle Swarm Optimization Algorithm for Computationally Expensive Numerical Problems," *Applied Soft Computing*, vol. 66, pp. 232-249, 2018. *Crossref*, <https://doi.org/10.1016/j.asoc.2018.02.025>
- [17] K. Aravinth Raaj, B. Joel Sherwin, and S. Sabeetha Saraswathi, "Automated Detection of Abnormalities in Chest X-Ray Images Using Convolutional Neural Networks," *International Journal of P2P Network Trends and Technology*, vol. 8, no. 2, pp. 18-24, 2018. *Crossref*, <https://doi.org/10.14445/22492615/IJPTT-V8I2P404>
- [18] Hui Xian Jaime Lin et al., "Remdesivir in Coronavirus Disease 2019 (Covid-19) Treatment: A Review of Evidence," *Infection*, vol. 49, no. 3, pp. 401-410, 2021. *Crossref*, <https://doi.org/10.1007/s15010-020-01557-7>
- [19] Sina F. Ardabili et al., "Covid-19 Outbreak Prediction with Machine Learning," *Algorithms*, vol. 13, no. 10, p. 249, 2020. *Crossref*, <https://doi.org/10.3390/a13100249>
- [20] Zeynep Ceylan, "Short-Term Prediction of COVID-19 Spread Using Grey Rolling Model Optimized by Particle Swarm Optimization," *Applied Soft Computing*, vol. 109, p. 107592, 2021. *Crossref*, <https://doi.org/10.1016/j.asoc.2021.107592>
- [21] Ivana Strumberger et al., "Designing Convolutional Neural Network Architecture by the Firefly Algorithm," *2019 International Young Engineers Forum (YEF-ECE)*, IEEE, pp. 59-65, 2019. *Crossref*, <https://doi.org/10.1109/YEF-ECE.2019.8740818>